IEEE Access
Multidisciplinary | Rapid Review | Open Access Journal

Date of publication xxxx 00, 0000, date of current version xxxx 00, 0000.

Digital Object Identifier 10

Extending Randles's Battery Model to Predict Impedance, Charge-voltage, and Runtime Characteristics

RAHAT HASAN[1] (Student Member, IEEE) JONATHAN SCOTT[2], (Senior Member, IEEE)
[1]School of Engineering, the University of Waikato, Hamilton, New Zealand (e-mail: rh163@students.waikato.ac.nz)
[2]School of Engineering, the University of Waikato, Hamilton, New Zealand (e-mail: jbs@waikato.ac.nz)

Corresponding author: Rahat Hasan (e-mail: rh163@students.waikato.ac.nz).

This work was supported in part by RH Innovation Limited and by WaikatoLink Limited.

ABSTRACT The impedance of a battery can be modelled with an elegant fractional-capacitor or "constant phase element" (CPE) equivalent circuit and a series resistor. In this manuscript, we present new evidence that suggests that a linear model similar to Randles' comprised solely of this impedance network is able to predict both the charge-voltage relationship epitomised by the familiar hysteresis curve of voltage as a function of charge as a battery charges and discharges through its linear region, and the recovery or "equilibration" transient that results from a step change in load current. The proposed model is unique in that it does not contain a source, either voltage or current, nor any purely reactive elements. There are important potential advantages of a passive battery model.

INDEX TERMS rechargeable battery, lithium-ion battery, state of charge, fractional modelling.

I. INTRODUCTION

THE literature reveals hundreds of papers in recent decades with the phrase "battery model" in the title, while thousands can be found on the subject in general in the IEEE stable alone. A battery model is considered key to prediction of behaviour, including state-of-charge (SoC) [1]–[5]. Readers not already familiar with the state of the art are directed to [1] which provides a broad literature review and an excellent summary of the various approaches including open-loop sensing based on open-circuit voltage (OCV) or Coulomb counting (CC) methods, and closed-loop state estimation using either a "black box" or equivalent-circuit. Further, some detail in the case of equivalent-circuit approaches were presented in [6]. In the preferred case of an equivalent-circuit model, the circuit is invariably a voltage source with a network of elements fitted to the apparent impedance of the cell [2], [6]. We might describe these as "Thévenin-like RC" models. Figure 1 depicts the popular first- and second-order examples of this type. More applications of a second-order "Thévenin-like RC model appeared in [7], [8] which is preferred by researchers than its predecessor when characterising cell SoC due to the extra degree of freedom. We have shown elsewhere that such models are theoretically unsuitable for modelling the runtime characteristics of a cell [9], [10].

More models in the last few years have returned to the use of fractional-derivative elements, mostly fractional capacitors, also known as Constant-Phase Elements or CPEs. A fractional element was reported by Randles in 1947 [11] in a equivalent-circuit model. The paper investigated rapid electrode reactions with a electrode system shown in figure 2. In Randles' model, Cl represents capacitance in the absence of electrochemical phenomena, and is small enough that it only comes into play at higher frequencies. It is what might be called "parasitic capacitance" in the electronic world. Cr, on the other hand, is a capacitive element with the angle fixed to 45 degrees. This non-ideal element was later introduced in [12] as a Warburg element. The basic form of Randles model for low frequencies is of a resistor in series with a Warburg element.

More recently, fractional derivatives were used in [13] and [14], but in a mathematical approach rather than through an equivalent circuit. Equivalent-circuit models incorporating fractional capacitors and Warburg elements have also appeared with varied success in [15]–[18].

This manuscript rests on certain key observations made in [19]. The impedance of a battery must be examined (and modelled) across the whole frequency range of signals to

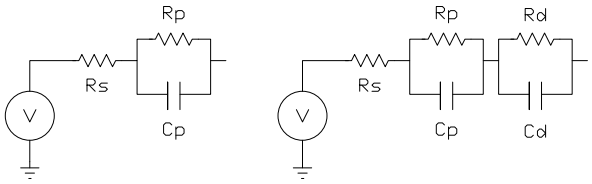

FIGURE 1.
Thévenin-style first- and second-order RC battery models.

which it is subjected; for a typical battery application with daily or less frequent recharging, this will run from a period of at least a day and quite possibly longer, to less than 1 second. This corresponds to a frequency span commencing no higher than 10μHz. Few authors venture below 1mHz for practical reasons, and some instrument setups give inaccurate impedance results in the case of fractional systems at low frequencies.

Drawing on the impedance results, a "R-CPE" model was presented in [19] for a Lithium-ion battery which follows Randles' model for lower frequencies, following the exception of a CPE angle which is now approximately 76 degrees. Although the model does a reasonable job of predicting the battery impedance, it is not perfect, and no attempt was made to investigate recovery transients and voltage hysteresis. Recent work described in [20] has shown that critical decay tails observed on neural implant electrodes are only correctly reproduced in simulation when the physically distributed nature of the electrodes is accounted for by "splitting" the CPE that represents the interface in the equivalent-circuit model. The splitting accounts for the distributed nature of the structure; the battery has energy stored in chemical species whose distance from the conducting plates varies. The split-CPE model is shown in figure 3, reproduced from [19]. The whole idea of an equivalent-circuit model is that you can relate voltage and current as functions of time, and simultaneously know about stored charge and energy. The new model perfectly fits the measured data in frequency domain as can be seen in figure 4. This manuscript now addresses the question of whether the split-CPE impedance model of [19] can predict working current, voltage, charge and energy.

II. INTRODUCTION TO FRACTIONAL CALCULUS

Many scientific and engineering communities remain unaware of fractional calculus. The most common reason for that is the lack of practical application; fractional calculus is often considered as a conceptual area that is of interest only to mathematicians. However, applications of fractional calculus have emerged in the areas of physics, biology and engineering [21]–[23]. Fractional calculus can provide simpler and more faithful models of physical systems that depend upon diffusion or that possess fractal properties. Such a model tends to provide "more entropy compared to its integer order counterpart with same number of parameters" [24], which is to say that it requires fewer parameters.

Fractional calculus was first defined by Liouville, Riemann and Grunwald in 1834, 1847 and 1867, respectively [25]. The Riemann-Liouville fractional-order derivative, preferred in engineering for causality reasons, is of the form:

$$\frac{d^{\alpha}v(t)}{dt^{\alpha}} = \frac{1}{\Gamma(1-\alpha)}\frac{d}{dt}\int_0^t (t-\tau)^{-\alpha}v(\tau)d\tau \qquad (1)$$

where Γ is the well-known Gamma function and $0 < \alpha < 1$ is an arbitrary real value called the order. In the same way that the Gamma function provides a real interpolation between the values of the integer factorial function, this definition provides a continuous transformation that happens to yield the same result as conventional, integer-order differentiation for integer arguments. This work lay unused for a long time.

The lack of "any acceptable geometric and physical interpretation" of fractional-order calculus has been lamented before [27]. There have been attempts to provide geometrical and physical interpretations of fractional operators, see for example [26], [27]. In [26] the author claims to develop 'an understandable geometric interpretation' using a Cantor's fractal set. This may explain the discrete nature of the impulse response function of a fractional integral. Later, a fascinating physical interpretation of Riemann-Liouville and Caputo fractional-order derivatives in relation to the cosmic time and the individual time was proposed in [27]. We contend that this 'understanding' is not helpful in circuit terms. It may help a mathematician grasp the idea, but it gives no circuit insight. We thus need to rely upon a simple formulation that fortunately results for a fractional capacitor in the Laplace domain.

Considering a fractional capacitor to be an element whose branch current is a fractional derivative of the branch potential expressed as a function of time, applying the Laplace transform to (1) with zero initial conditions produces a

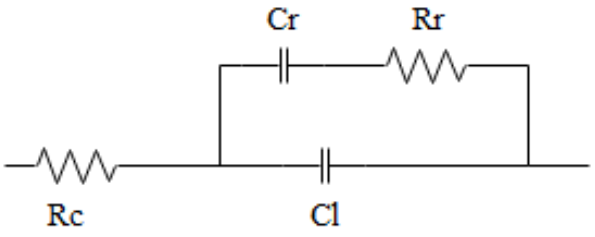

FIGURE 2.
Randles' equivalent-circuit model for rapid electrode reactions reproduced from [11].

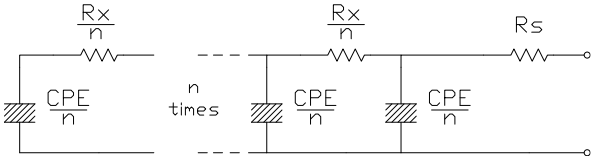

FIGURE 3. Equivalent circuit model with n-way split CPE and series resistance. The model requires four parameters, the order α and value C_F of the CPE, the series Resistance R_S and the splitting Resistance R_X, provided n is "sufficiently large".

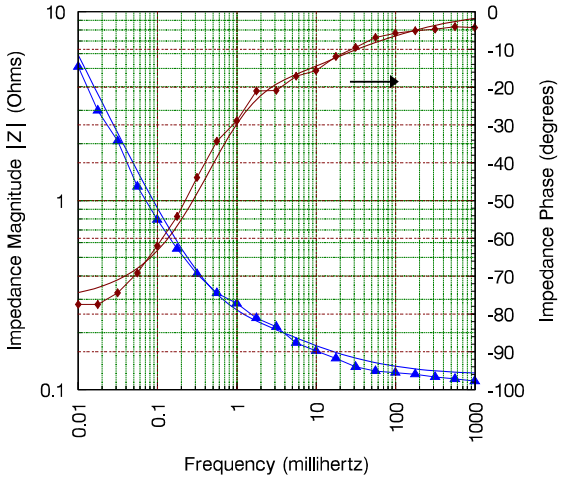

FIGURE 4. Impedance magnitude (left vertical axis, blue traces) and phase (right axis) of a 14500 Lithium-ion battery for frequencies corresponding to periods from 1 second to 1 day. Measured data (symbols) are compared with simulations using the split R-CPE model from [19]. The split-CPE equivalent circuit is reproduced in figure 3.

fractional-order function which portrays the current-voltage relationship of fractional capacitors:

$$I(s) = Cs^{\alpha}V(s) \tag{2}$$

Re-arranging the above equation gives the impedance of a fractional capacitor (CPE) in a form more familiar to circuit theorists:

$$Z(s) = \frac{V(s)}{I(s)} = \frac{1}{C_F s^{\alpha}} \tag{3}$$

where C is the "capacitance" of the fractional capacitor and α ranges between 0 and 1. The expression in (3) is perhaps the most compact and easily grasped representation of a CPE; it resembles a capacitor, but the slope of the impedance magnitude in a Bode plot will not quite be right; it will be $-\alpha$ instead of -1. Referring back to figure 4, it is straightforward to observe that at the very lowest frequencies a capacitor-like impedance characteristic appears. One then observes that the slope of the straight part is more like -0.85 than -1, implying that the "capacitor" is fractional.

III. CONSTRUCTING A CPE IN SPICE

As CPE rely on a fractional derivative, they are not routinely available as branch elements in compact simulators. Nevertheless, it is possible to generate a compact SPICE subcircuit that approximates the impedance of a CPE with arbitrary accuracy. The theory leading to the approximation is attributed to Morrison [28]. The data from the battery impedance in figure 4 permits the magnitude and angle of the CPE to be determined and a SPICE subcircuit generated as described in [29], with corrections from [30]. Two parameters are required to specify a CPE, corresponding to C_F and α from equation 3. For the Morrison formulation, these are a slope parameter, m, and a magnitude parameter found from a measurement of CPE admittance, Y_θ, at some arbitrary frequency, ω_0. Here the slope parameter m is found by observing that the CPE phase settles to 77.5 degrees or 1.35 radians around 10–20μHz, giving

$$m = \frac{\pi}{2\theta_{CPE}} = 1.161 \tag{4}$$

The CPE impedance is found from the measured impedance of the cell in the straight-line region at the low-frequency extreme. This gives values of 1.188Ω at 55.7μHz, yielding

$$Y_\theta = 0.842 \tag{5}$$

for $\omega_0 = 55.7 \times 10^{-6}$. An accuracy parameter of $k = 1.3$ is found to be more than adequate by trial and error.

IV. PREDICTING TRANSIENT RECOVERY

In this section, we will show that our proposed impedance network predicts more precisely the transient recovery of a battery. The measured tail of a single 800mAh, 14500 lithium battery is compared with various simulated tails. The test sequence consists of subjecting the cell to an isolated current pulse of 60 seconds, and the overall response is reproduced in the inset within the figure. The measurements were made with an Agilent E5270 Precision IV Analyzer and an Agilent 34401A DMM. All measurements were made with the battery held at a constant environmental temperature of 25 Celsius using a Contherm Polar 1000. Figure 5 shows the measured recovery transient of the same battery whose impedance appears in figure 4.

If we assume that for sufficiently low frequencies, the battery impedance is dominated by a CPE we can write

$$I(t) = C_F \frac{d^{\alpha}V(t)}{dt^{\alpha}} \tag{6}$$

or in the Laplace domain

$$Z_{batt} \approx Z_{CPE} = \frac{1}{C_F s^{\alpha}} = \frac{1}{C_F} s^{-\alpha} \tag{7}$$

The battery voltage recovery tail resulting from a square current pulse of period T and amplitude I_0 can be estimated by considering the current pulse to be the sum of two equal-sized step functions u, so that

$$I(t) = I_0 u(t) - I_0 u(t - T) \tag{8}$$

whose Laplace transform is

$$I(s) = \frac{I_0}{s} - \frac{I_0}{s} e^{-Ts} \tag{9}$$

thence

$$V(s) = \frac{I_0}{C_F} s^{-(1+\alpha)} - \frac{I_0}{C_F} s^{-(1+\alpha)} e^{-Ts} \tag{10}$$

Noting that the inverse Laplace transform

$$\mathcal{L}^{-1}(s^{-k}) = \frac{t^{k-1}}{\Gamma(k)} \tag{11}$$

putting $k = 1 + \alpha$, some algebra leads to an expression for the pulse voltage tail

$$v_{\text{Eq}}(t) = \frac{I_0}{C_F \Gamma(1+\alpha)} \left[t^{\alpha} - (t+T)^{\alpha} \right] \tag{12}$$

It is worth emphasizing that the voltage tail that follows a current pulse stimulus applied to a CPE, as given by (12), decays unusually slowly. It is remarkably different from a first or second-order conventional, exponential decay curve.

Returning to the recovery tail in figure 5, note that the first- and second-order Thévenin-style RC circuit models cannot fit the measured data, even when allowed to optimise freely, but the solid blue line predicted from the fitted split-CPE model comes much closer and has the correct curvature. The value of the splitting parameter R_X has been numerically optimised to obtain the best fit. In this case, we chose a value $R_X = 29\text{m}\Omega$. A 10-way split, that is $n = 10$, was chosen, again by trial and error observing that larger values conferred little advantage. Figure 6 plots the difference between each of the three predictions and the measured data. The new split-CPE model can predict the measured data with less than 3% error whereas, the percentage error of a single-RC and two-RC models is around 7% and 5.6% respectively. It is clear that the split-CPE model achieves considerably better an approximation with no more complexity than a first-order RC model.

V. CHARGE/VOLTAGE CHARACTERISTIC

The problem with measuring a battery charge-voltage characteristic is that this is a dynamic measurement. When charging a cell, the terminal voltage will be higher than would be the steady-state voltage perceived if the battery were completely at rest. A common response to this is to measure the voltage of the cell under constant-current charging and then to discharge at the same constant current, relying on the impedance characteristic to be linear and symmetrical. The steady-state characteristic is then approximated by averaging the two data sets point by point to yield the average characteristic. A very similar, but more informative, variant is used here.

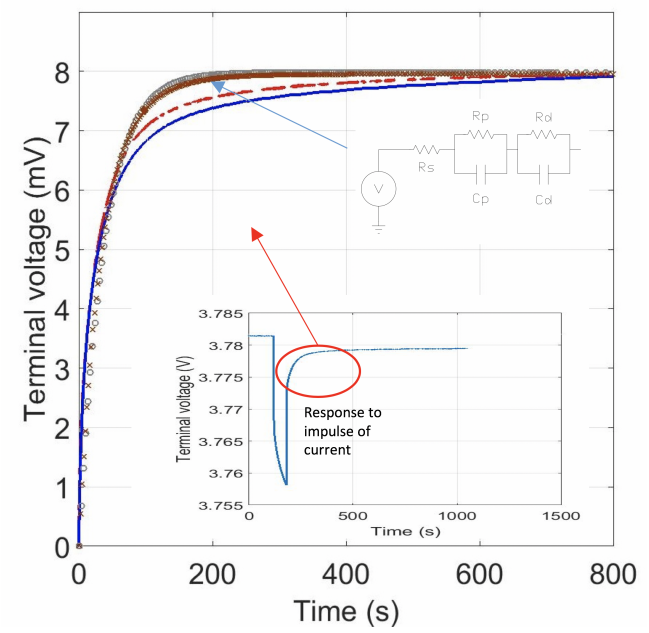

FIGURE 5. The response tails of a split-CPE model (solid line), one RC (○) and two RC (×) network models shown with measured data (dashed red line). Inset shows the full voltage response of the battery to a 60-second, 100mA pulse of load current and indicates the region where the "tail" appears.

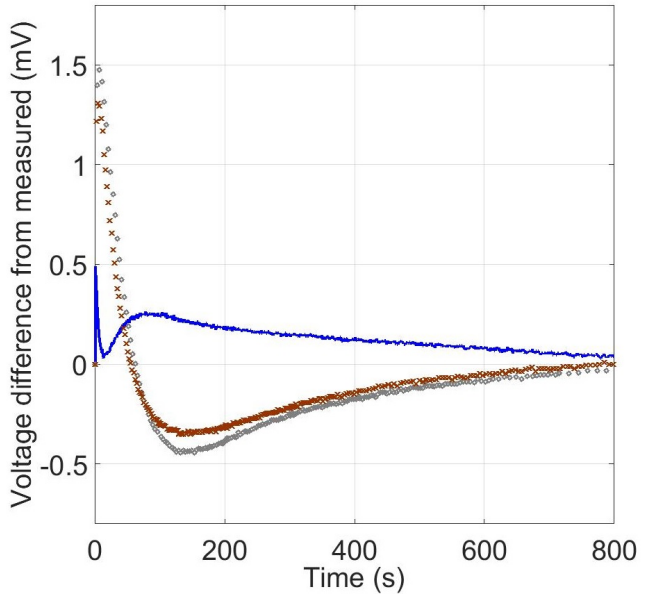

FIGURE 6. Voltage difference between measured data and single-RC (○), two-RC (×), and split-CPE (solid blue line) predictions presented in figure 5.

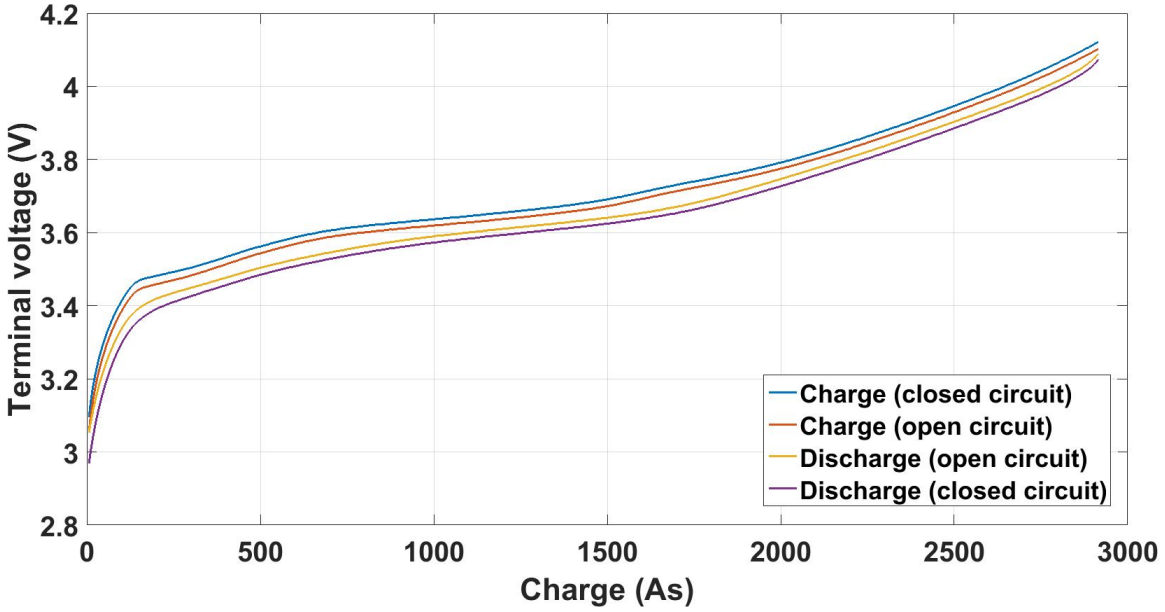

FIGURE 7. Voltage-charge characteristic of the 14500 Lithium-ion battery. Open-circuit trace voltages are measured after a 60-second rest, closed-circuit ones with current flowing.

The battery was charged at 100mA for 60 seconds using the E5270. Then the voltage was measured, the current set to zero for 60 seconds, and the voltage measured again. Reference to the measured data trace in figure 5 will indicate that 60 seconds should allow the battery to settle only some of the way towards its asymptotic value, owing to the exceptionally slow decay of the fractional tail. This cycle was repeated until the battery reached full charge. At the end of a sweep the battery was rested for 12 hours to allow equalisation. Next the current was set for discharge, and the same minute-off, minute-on scenario used to discharge the battery. Figure 7 shows four traces, being the charge and discharge characteristics during current flow ("closed circuit") and after the 60-second rest ("open circuit"). The steady-state characteristic is calculated by averaging the traces point by point. This is shown in figure 8.

Battery models are most usually sought to relate terminal voltage to SoC. The reader should note that the split-CPE model has been fitted to data obtained only from impedance and short-term dynamic response of the subject cell. The question arises as to how it will predict the charge-voltage characteristic of the cell. The simulated voltage trace in figure 8 was produced using SPICE with suitably-selected initial conditions. The fit is extraordinary as shown in figure 9, considering that the model was fitted without reference to the data of figure 7 except to obtain the dc offset.

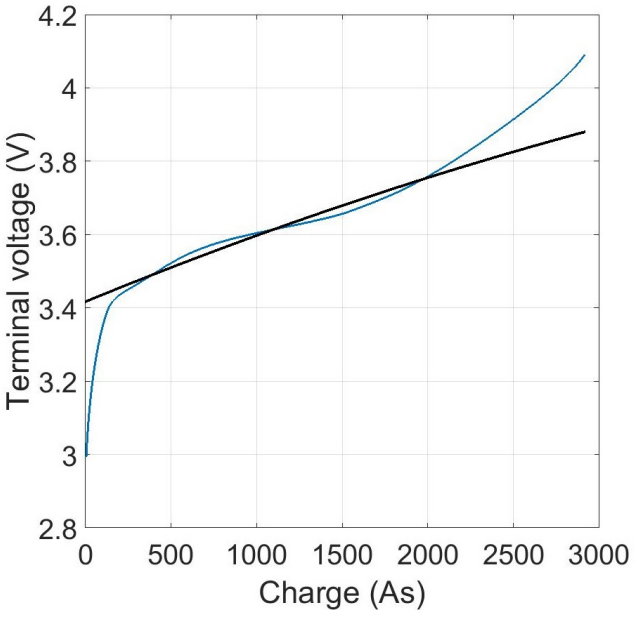

FIGURE 8. The estimated steady-state cell voltage obtained by averaging the traces from figure 7 (curved trace) is plotted against the voltage predicted by the split-CPE model (straight line).

VI. OTHER CHEMISTRIES

The model is not restricted to Lithium chemistry. In this section the split-CPE model is fitted to a Nickel-Metal Hydride cell type 55123 with 1850mAh nominal capacity. The present linear model is of limited use in the case of chemistries that permit float-current charging. This is because the model does not (yet) consider the "charge-dumping" process that effectively wastes energy as the energy-storing reactants deplete approaching the full-charge condition. We hope to extend the model to include the nonlinear "end effects" that shape the flat and full-charge ends of the characteristics. In the meantime, we seek to demonstrate that the idea of a passive

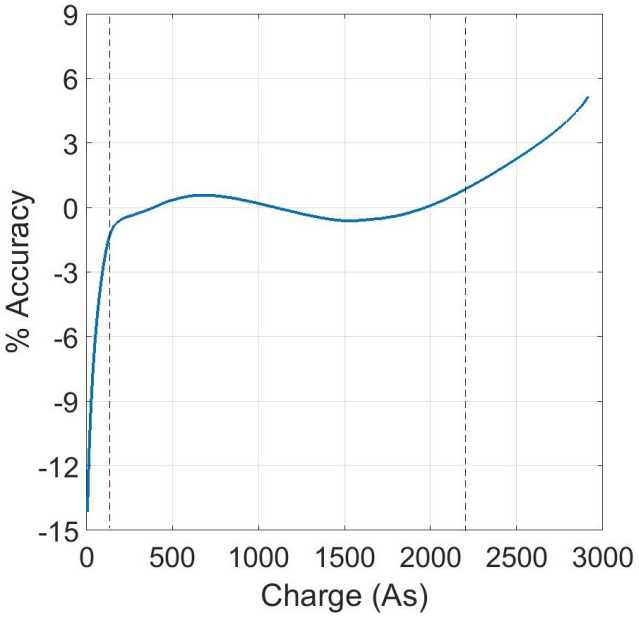

FIGURE 9. Plot of the percentage error between the measured and predicted traces shown in figure 8. The dotted lines mark the region within which error is less than 1%.

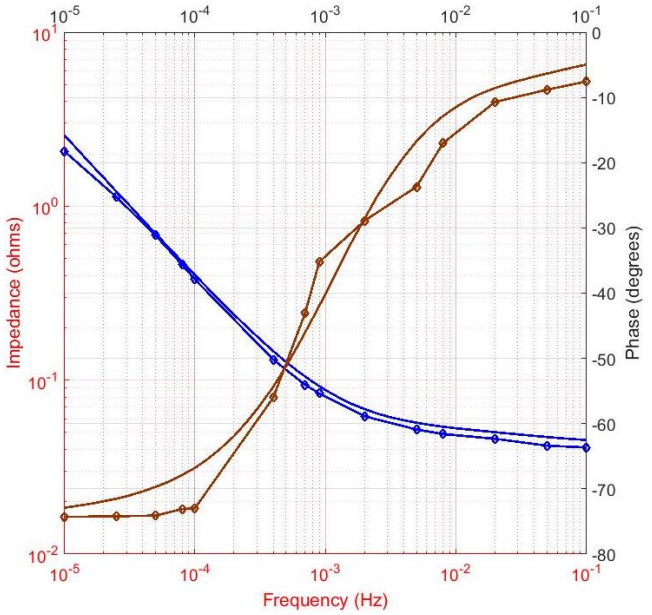

FIGURE 10. Measured (symbols) and simulated magnitude and phase of cell impedance for a single 55123 NiMH cell. Phase is the sigmoid curve, magnitude the hockey-stick curve.

model is not limited to the Lithium system.

The input data is as usual

1) a measurement of battery impedance versus frequency from which R_S and CPE parameters are obtained (figure 10);
2) the pulse response voltage recovery curve (figure 11); and
3) the characteristic of terminal voltage against charge measured in some particular fashion (figure 12).

The model is optimised to match the measured data, starting with values obtained from the impedance-frequency data. Simulated data obtained with SPICE using the method outlined in [29] with corrections from [30] and the fitted model parameters appear in figures 10, 11 and 12. The fit is sufficient for practical applications.

VII. DISCUSSION

A. BATTERY OPERATING RANGE

Battery manufacturers choose charge and discharge voltage points that are as far apart as possible in order to have the largest possible specified capacity. Thereafter the recommendation is to stay within a range such as 20–90% SoC for maximum life. For example, a Prius hybrid tries to keep its battery between 40% and 80% SoC to give long battery life [31]. The model proposed here is entirely linear; it makes no attempt to model the nonlinear subtleties of the voltage characteristic of figure 8. Nevertheless, reference to figure 9 shows that even without taking the nonlinearity of the voltage-charge characteristic into account, the model is accurate to a few percent from about 10% SoC to 90% SoC. The fuel gauge of a petrol car provides a measure that is only

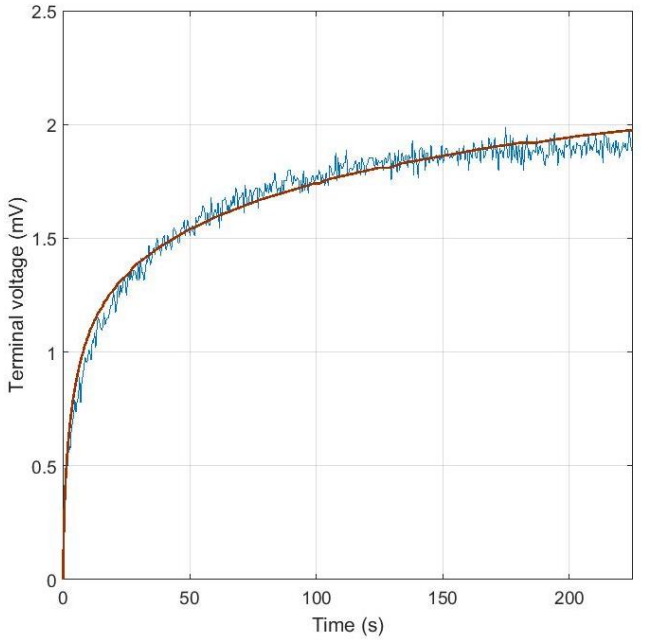

FIGURE 11. Measured (noisy trace) and simulated normalised recovery curve of the single 55123 NiMH cell following a 100mA current pulse of 90 seconds duration. The minimum terminal voltage is subtracted to leave only the change in terminal voltage after cessation of the pulse, i.e., the plot shows only the slow recovery.

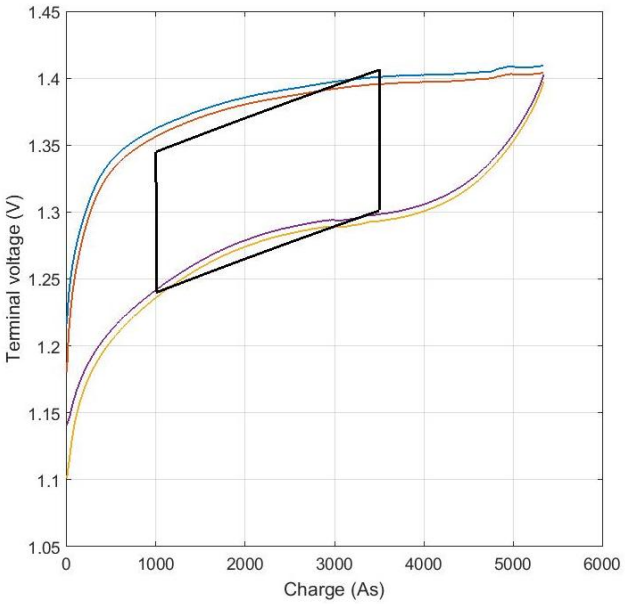

FIGURE 12. Measured (curves) and simulated (box) characteristic of a single 55123 NiMH cell charged and discharged in 60-second bursts spaced 120 seconds apart. Inner and outer curve pairs are the voltage at the ends of the 60-second periods of loading and the 120 seconds of rest at zero current, respectively.

accurate to about 5%, and while portable devices read out battery status to 1% most users notice that they are not that accurate and prone to sudden large corrections. The authors submit that the linear model may already be sufficient for many practical uses.

B. NONLINEAR EXTENSION

Nevertheless, extension to predicting the subtle nonlinear curves visible in an actual battery characteristic such as figure 7 is expected to be possible. The approach favoured by the authors involves modelling the reduction of chemical species at the electrode interface by way of charge-dependent capacitances in the CPE subcircuit through the magnitude parameter of the CPE, Y_θ [29]. This approach is easy to incorporate in nodal simulators, and has a strong physical basis in the modelling of species concentrations at an electrode interface through the general form of the Butler-Volmer equation [32]. This extension is considered to be beyond the scope of this manuscript, but is the logical next step.

C. EFFICIENCY

The model contains no sources, and can thus neither add nor subtract energy in an arbitrary fashion—just as in the case of a rechargeable battery. We expect the lossy CPEs will model the energy difference between that supplied in charging and that obtained in discharge. Thus a collateral benefit of this compact model is expected to be the ability to straightforwardly calculate the efficiency of energy storage for any scenario, i.e., it will predict how much of the energy invested in charging is returned in the discharge phase for an arbitrary dynamic load. An investigation of the model's accuracy in predicting the efficiency of energy return is considered out of the scope of this manuscript, but is being addressed separately.

VIII. CONCLUSION

This manuscript extends Randles' model to low frequencies to characterise behaviour of a Lithium-ion cell. The modified model is now simple and contains only a series resistor and a CPE with an angle that varies with cell chemistry. It also does not require any voltage or current sources. Although, the work reported here is carried out with single Lithium-ion and NiMH cells but it is applicable to all cell types. It is clear that such a model is superior to existing, complex models that do not seem to add anything for their extra parameters.

To further investigate the model's ability to predict recovery or hysteresis which most authors do not check, the CPE in the model is arbitrarily divided into smaller CPEs to account for the distributed nature of the electrodes. Now with only 4 parameters, it can accurately estimate the battery's runtime transient characteristics and the variation of voltage with state-of-charge in the "linear" range within a few percents. The new split-CPE model also fits the impedance-frequency data better.

Such a model is expected to exhibit very powerful properties. The possibility exists to extend the model in the future into the end regions where the voltage becomes a strongly non-linear function of available charge. The absence of a voltage or current source means that the model can be used to calculate the efficiency of energy stored in a cell that has not been proposed previously.

REFERENCES

[1] Jufeng Yang; Bing Xia; Yunlong Shang; Wenxin Huang; Chunting Chris Mi, "Adaptive State-of-Charge Estimation Based on a Split Battery Model for Electric Vehicle Applications", IEEE Transactions on Vehicular Technology, 2017, Volume: 66, Issue: 12, pp. 10889 - 10898.

[2] G. Nobile, M. Cacciato, G. Scarcella, and G. Scelba, "Performance Assessment of Equivalent-Circuit Models for Electrochemical Energy Storage Systems", 43^{rd} Annual Conference of the IEEE Industrial Electronics Society (IECON), 2017, pp2799–2806.

[3] Dinh Vinh Do, Christophe Forgez, Khadija El Kadri Benkara, and Guy Friedrich, "Impedance Observer for a Li-Ion battery using Kalman filter", IEEE Transactions on Vehicular Technology, vol. 58, no. 8, pp. 3930–3937, Oct. 2009.

[4] Hicham Chaoui, Navid Golbon, Imad Hmouz, Ridha Souissi, Sofine Tahar, "Lyapunov-based adaptive State of Charge and State of Health estimation for Lithium-ion batteries", IEEE Transactions on Industrial Electronics, Volume: 62, Issue: 3, 2015, pp.1610–1618.

[5] Arijit Guha, Amit Patra, "Online estimation of the Electrochemical Impedance Spectrum and Remaining Useful Life of Lithium-ion batteries", IEEE Transactions on Instrumentation and Measurement, 2018, Vol. 67, Issue. 8, pp. 1836 - 1849.

[6] Cheng Zhang, Kang Li, Sean Mcloone, and Zhile Yang, "Battery Modelling Methods for Electric Vehicles — A Review", European Control Conference (ECC), Strasbourg, France, June 24–27, 2014.

[7] Liu, K., Hu, X., Yang, Z., Xie, Y., Feng, S., "Lithium-ion battery charging management considering economic costs of electrical energy loss and battery degradation", Energy Conversion and Management, 2019, 195, 167–179.

[8] Kailong Liu, Changfy Zou, Kang Li, Torsten Wik, "Charging Pattern Optimization for Lithium-Ion Batteries with An Electrothermal-Aging Model", IEEE Transactions on Industrial Informatics, 2018, 1–1.

[9] Hasan, R., Scott, J. B., "Measurement for fractional characteristic of lithium batteries", 2019 IEEE International Instrumentation and Measurement Technology Conference, Auckland, New Zealand, 2019.

[10] Hasan, R., Scott, J. B., "Application of Swingler's Method for Analysis of Multicomponent Exponentials with Special Attention to Non-equispaced Data", 2016 IEEE 12th International Colloquium on Signal Processing & Its Applications (CSPA), 4-6 March 2016, Malaysia, pp. 12–15.

[11] J. E. B. Randles, "Kinetics of rapid electrode reactions," Discussions of the Faraday Society, 1:11, 1947.

[12] Grimnes, S. and O. Martinsen, Bioimpedance and bioelectricity basics. 2008: Academic Press.

[13] Mikal Cugnet, Jocelyn Sabatier, Stephane Laruelle, Sylvie Grugeon, Bernard Sahut, Alain Oustaloup, and Jean-Marie Tarascon, "On lead acid battery resistance and cranking-capability estimation", IEEE Transactions on Industrial Electronics, Vol. 57, No. 3, March 2010, pp. 909–917.

[14] Jocelyn Sabatier, Mathieu Merveillaut, Junior Mbala Francisco, Franck Guillemard, Denis Porcelatto, "Fractional models for lithium-ion batteries", 2013 European Control Conference (ECC), Zurich, Switzerland, July 2013, pp. 3458–3463.

[15] Yan Ma, Xiuwen Zhou, and Hong Chen, "Fractional modeling and SOC estimation of Lithium-ion battery", IEEE/CAA Journal of Automatica Sinica, Vol 3, No. 3, July 2016, pp. 281–287.

[16] Scott, J. B., & Hasan, R., "Letter to the Editor Re 'Fractional Modeling and SOC Estimation of Lithium-ion Battery'." IEEE CAA Journal of Automatica Sinica, 5(2), pp644–644, 2018.

[17] Qian-Kun Wang, Yi-Jun He, Jia-Ni Shen, Xiao-Song Hu, Zi-Feng Ma, "State of Charge-Dependent Polynomial Equivalent Circuit Modeling for Electrochemical Impedance Spectroscopy of Lithium-Ion Batteries," IEEE Transactions on Power Electronics, Vol. 33 , no. 10, 2018, pp8449–8460.

[18] Hasan, R., & Scott, J. B., "Comments on 'State of Charge-Dependent Polynomial Equivalent Circuit Modeling for Electrochemical Impedance Spectroscopy of Lithium-Ion Batteries'." IEEE Transactions on Power Electronics, 1–1, 2019.

[19] Scott, J.B. and Hasan, R., "New Results for Battery Impedance at Very Low Frequencies", IEEE Access, vol. 7, 30 July 2019, pp106925–106930. DOI 10.1109/ACCESS.2019.2932094.

[20] P. Single and J. Scott, "Cause of pulse artefacts inherent to the electrodes of neuromodulation implants", IEEE Trans. Neural Syst. Rehabil. Eng., vol. 26, no. 10, pp. 2078–2083, Oct. 2018.

[21] Hilfer RJ. (Ed.), "Applications of Fractional Calculus in Physics", World Scientific, Singapore, 2000.

[22] Richard L. Magin, "Fractional calculus models of complex dynamics in biological tissues", Computers and Mathematics with Applications, 59 (2010), 1586–1593.

[23] Clara M. Ionescu, J. A. Tenreiro Machado, and Robin De Keyser, "Modeling of the Lung Impedance Using a Fractional-Order Ladder Network With Constant Phase Elements", IEEE Transactions on Biomedical Circuits and Systems, vol. 5, no. 1, February 2011.

[24] Avishek Adhikary, Pritin Sen, Siddharha Sen, and Karabi Biswas, "Design and Performance Study of Dynamic Fractors in Any of the Four Quadrants," Circuits Systems and Signal Processing, (2016) 35:1909–1932.

[25] I. Podlubny, "Fractional differential equations", Academic Press, 1999.

[26] M. Moshrefi-Torbati and J. K. Hammond, "Physical and Geometrical Interpretation of Fractional Operators," Journal of the Franklin Institute, Vol. 3358, No 6, pp.1077–1086, 1997.

[27] Igor Podlubny, "Geometric and Physical Interpretation of Fractional Integration and Fractional Differentiation", Fractional Calculus and Applied Analysis, vol. 5, no. 4, 2002, pp.367–386.

[28] R. Morrison, "RC constant-argument driving-point admittances", IRE Transactions on Circuit Theory, vol. 6, no. 3, pp310–317, September 1959.

[29] Jonathan Scott and Peter Single, "Compact Nonlinear Model of an Implantable Electrode Array for Spinal Cord Stimulation (SCS)", IEEE Transactions on Biomedical Circuits and Systems, vol.8, no.3, pp.382–390, 2014.

[30] Sinduja Seshadri and Jonathan Scott, "Correction to 'Compact Nonlinear Model of an Implantable Electrode Array for Spinal Cord Stimulation', [Jun 14, 382–390], IEEE Transactions on Biomedical Circuits and Systems, Volume:12, Issue:4, pages:963–964, 2018.

[31] Leijen, P., Steyn-Ross, D. A., & Kularatna, N. , "Use of Effective Capacitance Variation as a Measure of State-of-Health in a Series-Connected Automotive Battery Pack", IEEE Transactions on Vehicular Technology, 2018, 67(3), pp. 1961–1968.

[32] Daniel R. Merrill, Maron Bikson and John G. R. Jefferys, "Electrical stimulation of excitable tissue: design of efficacious and safe protocols", Journal of Neuroscience Methods 141 (2005), pp171–198.